

# Subsea Cable Search and Path Estimation using Graph SLAM for AUV-based Inspection

Ibrahim Fadhil Djauhari, Adrian Bodenmann, Samuel Simmons, and Blair Thornton  
University of Southampton, Southampton, UK  
ifd1n23@soton.ac.uk

**Abstract**—This research develops a method to efficiently search for and track subsea communication cables using an Autonomous Underwater Vehicle (AUVs). Inspection of subsea communication cables is a challenging task because they are narrow, making them difficult to detect, have significant route uncertainty that increases with depth, and can be buried for part of their length. The method is based on Simultaneous Localisation and Mapping (SLAM) using an initial map of the cable path that is assumed to be uncertain. Map-guided search patterns are first generated, where successful cable observations update the map using graph-based SLAM. We address the correspondence problem by defining a cable-relative coordinate frame that allows observations to be matched to map locations without the need for distinct cable features. Route uncertainty estimates are based on the location uncertainty of the AUV when observations are made, and physics-based catenary calculations for regions where the cable has not been observed. Updating cable route maps using this approach allows an AUV to efficiently recover a cable route even if it cannot be tracked for part of its length. Here we present the results of simulations that assume a camera-equipped AUV, and demonstrate robust performance of the method on five different cable routes, each with buried sections where the cable is undetectable and different initial cable route uncertainties.

**Index Terms**—AUV, subsea cable, map-guided search, inspection, cable tracking, SLAM, GraphSLAM

## I. INTRODUCTION

Subsea communication cables total more than 1.4 million kilometres in length and transmit over 95% of international data [1]. The majority of this length is at depths of over 1000 m, where cables are unburied and have diameters of less than 30 mm. Every year, there are reports of several hundreds of incidents where such cables are damaged due to both natural causes and human activities [2]. Among the various underwater vehicle technologies, Autonomous Underwater Vehicles (AUVs) have the potential to efficiently inspect the condition of these subsea cables due to their long operating range.

Subsea cable positions are mapped when the cables are first laid down on the seafloor. The mapped cable paths have initial position uncertainties of 5–10% of water depth due to impacts of underwater currents that cannot be perfectly modelled [3]. Over time, the subsea cables can get displaced from their initial positions due to currents and other disturbances, with offsets of 975 m from their original position being reported in [4]. Even at large depths where cables are typically laid directly

on top of the seafloor, cables can become partially buried under sediments, making them difficult to detect.

Various methods exist for AUVs to detect the small diameter of deep-sea communication cables. These include visually using cameras, electromagnetically using magnetometers, and acoustically using high-resolution imaging sonars. The measurement swath of such high-resolution sensors is typically smaller than the uncertainty of deep-sea cable routes, which makes traditional waypoint following ineffective. When a section of cable can be detected, AUVs can be programmed to track their length [5]. However, autonomous behaviours for when a cable cannot be detected are less well studied, with researchers proposing the use of zig-zag search patterns within some distance of the last detected cable point [6] or reverting back to some prior map of the cable until it can be found again [5]. Searching within a bounded area from the last successful cable detection may not be robust if the cable is partially buried and only emerges outside of the search area, and methods to determine an appropriate search area and direction need to be considered. Similarly, following a prior cable path lacks robustness if the prior map is inaccurate. The limitations can be addressed by updating cable path maps based on successful observations and using catenary calculations to bound search areas based on the curvature of a cable when subjected to disturbance.

Optimising the consistency of a cable route map with cable observations can be considered as a full-path Simultaneous Localization and Mapping (SLAM) problem. Robots often use SLAM to simultaneously construct a map of their surroundings and localise themselves within it. Although full SLAM typically optimise the entire path taken by the robot, here we optimise the entire path of a cable, which is initialised using a prior map [5]. Since underwater robots can self-localise with uncertainties less than 10% of depth (the uncertainty of cable route maps using standard navigational suites), successful cable detections can improve cable route estimates. Solving full SLAM using error minimisation techniques requires the correspondence between robot observations and features of a map to be determined. However, subsea cables are featureless, where a section of cable is typically indistinct from any other section of the same cable, making it difficult to correspond cable observations to specific parts of the cable in a path map. A method to determine this correspondence is needed to apply error minimisation-based SLAM for cable path estimation.

This paper develops an AUV cable inspection method that

This project is funded by the Defence and Security Accelerator (DASA). Data used for method development was gathered during the FK180731 cruise of the Schmidt Ocean Institute's R/V Falkor using the University of Tokyo AUV AE2000F.

generates search patterns based on cable route maps and maintains the map using graph-based SLAM. We introduce a novel cable relative coordinate frame to address the correspondence problem between observations and the cable map, then simulate the performance of the method using simulations of actual cable routes.

## II. METHOD

### A. Cable Coordinate Frame

A cable-relative coordinate frame is defined to enable feature-free correspondence between cable observations and different points along the cable length. The  $SE(2)$  cable coordinate frame  $\vec{F}_C$  (Fig. 1) is determined by fitting a first-order polynomial through points along the cable path in the initial map. The two axes of the cable coordinate frame are defined as *along* ( $x_C$ ), which represents the distance along the length of the cable in the initial map, and *normal* ( $y_C$ ), which represents the lateral displacement of the cable position from  $\vec{F}_C$  due to the cable's curvature. Although the actual cable route may deviate from the initial map, we assume these deviations will consist mainly of local offsets due to the currents that existed during cable lay operations and physical disturbances after the cable has been laid. The primary axis is assumed to be reasonably well-aligned. During an inspection, the AUV primarily moves in the positive *along* axis direction, and as long as the cable route does not loop in on itself, the distance travelled along the primary cable axis can be used to assign correspondence between observations and the map. In cases where the cable is expected to loop around so that the cable exists at multiple lateral offsets for the same distance along the primary axis, the problem can be addressed by defining the cable coordinate frame in shorter local sections.

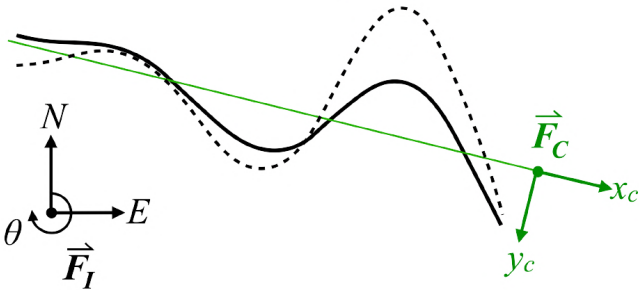


Fig. 1. Illustration of the cable coordinate frame  $\vec{F}_C$  and the North-East-Down (NED) frame  $\vec{F}_I$ . The solid and dotted black curve represents the prior and the actual cable path respectively. Although we expect local deviations between the actual and initially assumed cable routes, the proposed method is robust to small discrepancies as long as the primary axes are reasonably well aligned (i.e., not perpendicular to each other).

Fig. 2 shows how the cable coordinate frame is generated from a prior cable path in the North-East-Down (NED) frame. The centre point of the cable path is used as the origin of the cable coordinate frame. The transformation from NED to

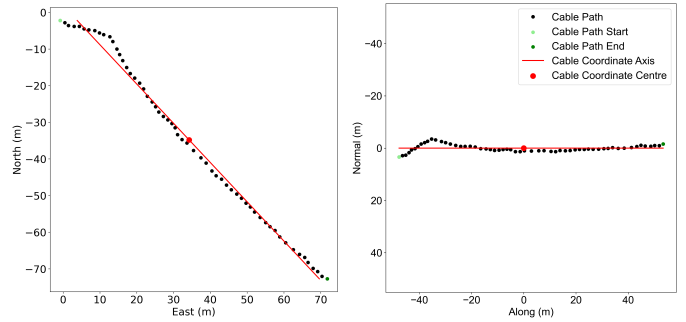


Fig. 2. A cable path in the NED (left) and cable coordinate frame (right). The red line is fitted using linear regression through each point in the cable path. The resulting line represents the *along* axis of the cable coordinate frame. The  $y$ -axis is inverted on the cable coordinate frame as illustrated by the  $y_C$  axis in Fig. 1. If actual cable route deviates from the assumed cable prior map, it is not problematic provided the directions of the primary axes of the actual and initially assumed cable routes are far from orthogonal.

cable frame is done by first translating the cable path by a distance of the cable coordinate centre point and rotating it by its bearing angle. The cable path extends in each direction with equal length in the *along* axis.

### B. Cable Path Estimation

Cable path estimation is formulated as a SLAM problem that starts with an approximate map of the cable route and its uncertainty (i.e., a prior map). We use GraphSLAM to represent the cable route, where the prior cable path is discretised into  $N$  points that form nodes in the graph. Every time the robot observes the cable, a new node is formed with its position uncertainty determined from the robot's pose uncertainty at the time of observation. Constraints are formed between nodes that have the same distance along the initial cable primary axis, which allows the graph to be optimised to determine the full cable path that is most consistent with cable observations [7].

When the AUV can detect the cable, it can track it directly using methods such as those described in [8]. When the AUV cannot detect the cable, any new observations are used to perform a SLAM update together with previous observations to optimise the consistency between the observations and the cable path subject to edge constraints. A comparison between a cable path before and after an update is shown in Fig. 3.

The update adjusts both the cable mean path estimate and its uncertainty. Fig. 4 shows an example for one observation, where the cable path is updated to maximise consistency with the observation, which has a far smaller uncertainty than the initial cable (blue) to the updated posterior (green), where the uncertainty shown represents  $3\sigma$ , and is used as a hard constraint on the AUV's search pattern. The uncertainty grows from observed cable locations where the rate of growth is constrained using cable catenary calculations. This represents the lateral region that the cable could be in based on assumed friction and cable load-bearing calculations [3]. Updating the cable path and uncertainty reduces the area that the AUV needs

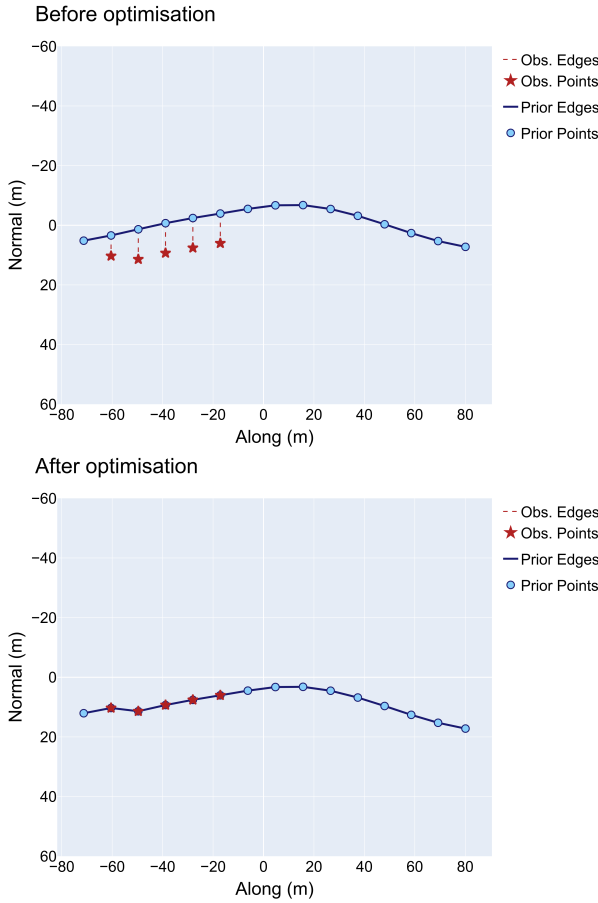


Fig. 3. Graph of a prior cable path before (top) and after (bottom) a SLAM update consisting of five observations. The SLAM update moved the entire cable path to the positive *normal* axis to be consistent with the observation positions. The shape of the cable path can still change due to shifts in individual cable points.

to search if it loses track of the cable, which in turn improves the overall inspection efficiency.

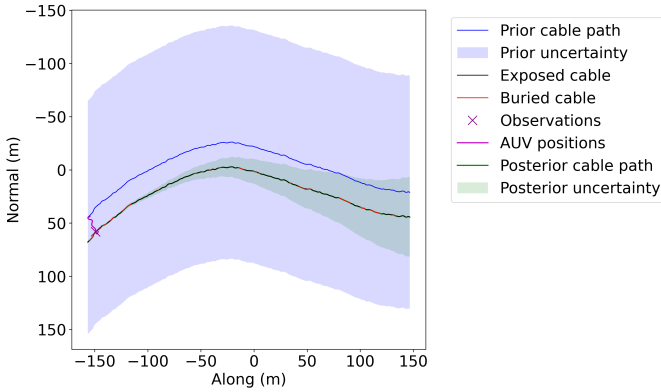


Fig. 4. The cable path position and uncertainty after a SLAM update. The AUV (purple) made one cable observation (purple cross) and updated the cable map. The posterior cable path (green) is on top of the ground truth cable and its uncertainty area shrank compared to the prior cable path (blue).

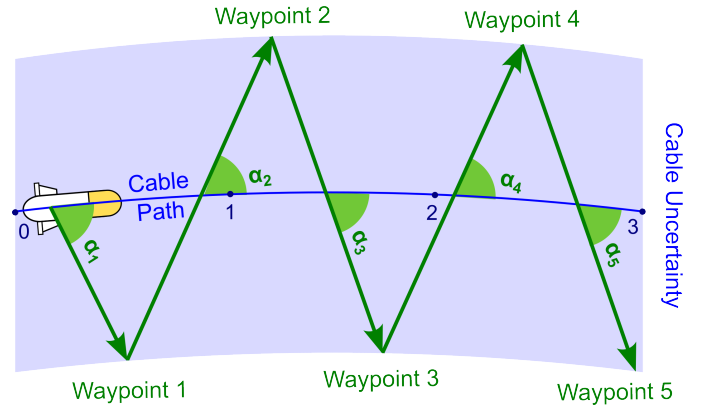


Fig. 5. Illustration of the cable search waypoint generation. The cable path consists of four discrete cable points from index 0 to 3. Five waypoints are illustrated with a search angle of  $\alpha$  leading from one end of the uncertainty boundary to the other.

### C. Cable Search

Various algorithms have been developed to track cable paths while the cable can be detected [8]. When the cable cannot be detected however, the AUV should search the area the cable is most likely to be. This is achieved based on a zig-zag search pattern [6] (illustrated in Fig. 5) that is bounded by cable catenary calculations and parametrised by the cable search angle  $\alpha$ , which is the angle between the map cable path and the AUV trajectory.

The cable search bearing angle  $\alpha$  can be formulated as:

$$\alpha = \text{sign} \cdot \text{search angle} + \text{cable bearing} \quad (1)$$

$$\alpha = \pm \Delta\alpha + \arctan\left(\frac{y_{i+1} - y_i}{x_{i+1} - x_i}\right) \quad (2)$$

where  $\alpha$  is the cable search bearing angle shown in Figure 5, *search angle* is a linearly parametrised search angle  $\Delta\alpha$ , and *cable bearing* is the bearing angle between the next ( $i + 1$ ) and current ( $i$ ) cable point. The angle  $\Delta\alpha$  linearly scales with the cable uncertainty up until a specified maximum search angle. The value of *sign* determines the direction of the search waypoint. The sign alternates between negative when the AUV is above the cable path, and positive when the AUV is below it on the *normal* axis. The alternating values ensure a waypoint will be created to the opposite end of the uncertainty boundary and form a zig-zag pattern as shown in Fig. 5.

If the AUV moves outside the bounded areas, a waypoint will be created at the nearest known cable point. This ensures that the AUV will return and continue its search within the uncertainty bounds.

## III. RESULTS

Subsea cable inspection using the proposed search and path estimation method is simulated for a camera equipped AUV, assuming an inspection speed of 0.25 m/s and search angle of  $70^\circ$ . The visual subsea cable detection and following system described in [8] is used in the simulation configured with perfect detection performance (0% false positives and 0% false

TABLE I  
PARAMETERS OF THE FIVE PRIOR CABLE PATHS

Path	Along Length (m)	Depth (m)	Initial Uncertainty (m)
1	101	775	77.5
2	135	775	77.5
3	303	775	77.5
4	153	15	1.5
5	151	15	1.5

TABLE II  
PARAMETERS OF THE BURIED SECTIONS OF THE FIVE PRIOR CABLE PATHS

Path	Number of Buried Sections	Percentage of Buried Cable (%)
1	2	20.1
2	10	30.9
3	9	25.9
4	1	25.9
5	2	30.1

negatives) where the cable is exposed on the seafloor, and a camera field-of-view of  $46^\circ \times 60^\circ$  operating at an altitude of  $1.5m$ . This gives each image frame an area of  $1.7 \times 1.3m$  on the seafloor in which it can detect the cable. We assume an image acquisition rate of 1 Hz.

The simulation uses five known subsea cable paths, where various displacements are added to generate prior cable paths, and buried sections where the cable cannot be observed are artificially introduced. Cable paths 1, 2, and 3 were mapped during the FK180731 survey using the AE2000F AUV at the Southern Hydrates Ridge, off Oregon [9]. Paths 4 and 5 are cable paths surveyed using the Smarty200 AUV at the coast of Plymouth in 2024. The five paths are shown in Fig. 6. The initial cable map uncertainty of each path is defined as 10% of its depth as described in Table I. Each cable path is then displaced by a Low, Medium, and High distance, which corresponds to lateral displacements of 30%, 60%, and 90% of the initial cable map uncertainty. Each test configuration is simulated five times.

Each path has between one and ten buried sections where the cable cannot be observed, to test the ability of the method to relocate the cable once it is exposed again. The number of buried sections and the percentage of buried sections in the cable path are shown in Table II. For paths 1 to 3, the buried cable sections are chosen based on cable images taken during the FK180731 survey. The sections classified as buried shown in Fig. 6 are sections where the surveyed cable images were obscured, partly buried, and/or in very low resolution. For paths 4 and 5, the buried sections are artificially chosen to simulate buried sections over longer stretches of the cable, while maintaining a similar total buried cable proportions of paths 1 to 3.

To measure the success of the simulated inspections, we define the efficiency of the AUV's observations as [8]:

$$\eta_{observed} = \frac{\text{Observed Cable Length}}{\text{Remaining Observable Cable Length}} \quad (3)$$

where "Observed Cable Length" refers to the length of cable observed by the AUV's cameras and "Remaining Observable

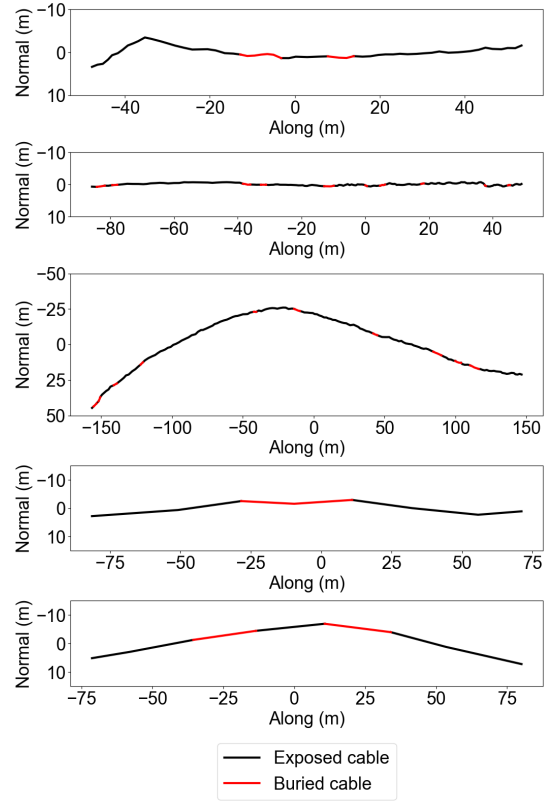


Fig. 6. The five ground truth cable paths used in the simulation. From top to bottom: paths 1, 2, 3, 4, and 5 in the cable-relative coordinate frame. Buried cable sections of varying length and complexity are added to each path.

Cable Length" refers to the length of observable cable that remains after the AUV finds the cable for the first time. This parameter ignores the initial distance the AUV needed to travel in order to find the cable, which depends on the search angle and initial cable uncertainty. Since these simulations assume perfect cable detection, the parameter represents how efficiently the AUV can relocate it after it loses tracking due to the buried section where the cable cannot be observed.

The results in Table III show that the AUV could consistently observe at least 66% of the remaining cable after making an initial observation. Since the method updates its map based on successful cable observations, the increased cable displacement from the prior map doesn't impact the observation efficiency results.

Fig. 7, shows an example of the results for cable path 3. The initial cable search crosses over the actual cable path due to a buried section of the cable. However, the search pattern turns back after reaching the uncertainty-driven search boundary and crosses a section of exposed cable on its way back. The initial observation shifts the posterior map to the true cable location, and the uncertainty grows in both the forward and backward reverse directions.

Fig. 8, shows an example of the results in cable path 5. As the AUV tracks the cable, the updated map allows the cable location to be quickly recovered after long sections of

TABLE III  
AVERAGE OBSERVATION EFFICIENCY ( $\pm$  STD. DEV.) AFTER THE INITIAL OBSERVATION IN FIVE CABLE INSPECTION SIMULATIONS OF THE FIVE PRIOR PATHS AT LOW, MEDIUM, AND HIGH CABLE DISPLACEMENT.

Cable Displacement	Observation Efficiency (%)				
	Path 1	Path 2	Path 3	Path 4	Path 5
Low	90.2 $\pm$ 4.6	82.24 $\pm$ 11	82.64 $\pm$ 3.4	75.72 $\pm$ 1.9	67.47 $\pm$ 2.5
Medium	79.77 $\pm$ 8.3	87.17 $\pm$ 5.9	78.73 $\pm$ 4	69.62 $\pm$ 2	70.44 $\pm$ 2
High	82.12 $\pm$ 5.8	78.89 $\pm$ 9.3	76.97 $\pm$ 8.7	72.86 $\pm$ 1.9	67.42 $\pm$ 3.4

buried cable are encountered. When the AUV moved outside the bounded area, it was guided back to the nearest prior cable point and continued its zig-zag search.

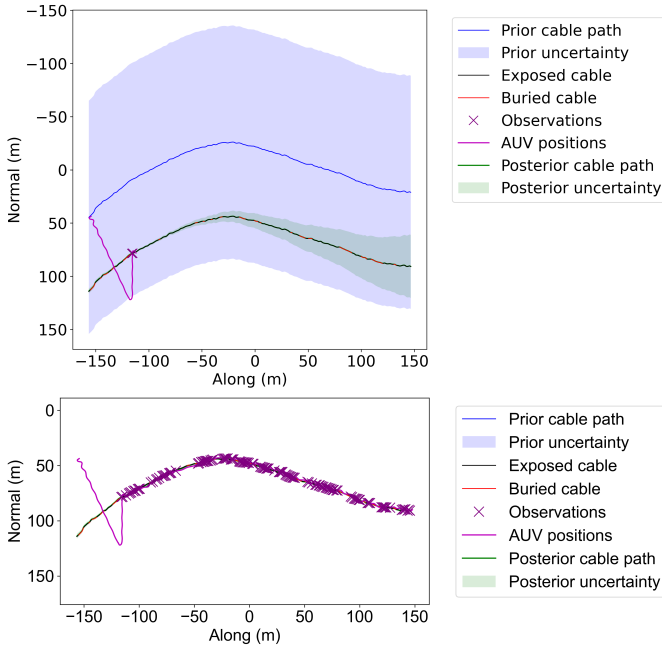


Fig. 7. AUV poses, observations, cable paths, and cable uncertainties after the first (top) and last (bottom) observation of the Path 3 search with high cable displacement.

#### IV. CONCLUSION AND FUTURE WORK

This paper proposes a method for AUVs to inspect subsea cables. The method assumes initial maps have position uncertainty, and uses SLAM to update the cable path to make them consistent with cable observations. Simulations show that the AUV can find the cable using a map and uncertainty-guided zig-zag pattern within a bounded area of the prior cable path. A cable-relative coordinate frame is introduced to match observed cables to corresponding areas of the map without relying on the distinctive features of the cable. The uncertainty of the cable paths in regions that have not been observed can be determined using catenary calculations to narrow down the search region in a principled manner.

This allows an AUV to observe consistently high proportions of the remaining cable length after making an initial

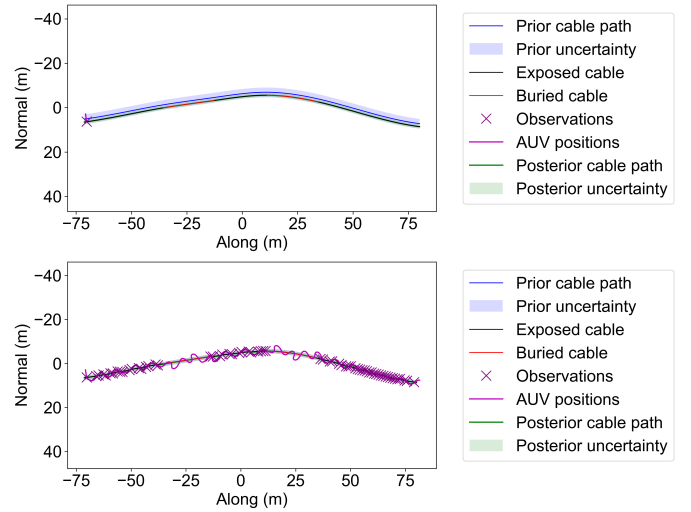


Fig. 8. AUV poses, observations, cable paths, and cable uncertainties after the first (top) and last (bottom) observation of the Path 5 search with high cable displacement.

observation despite there being numerous buried sections in the remainder of the cable. In the simulations, we assumed perfect cable detection, however, the behaviour would also recover the cable path in situations where the cable cannot be tracked temporarily due to imperfect detection.

Future work to increase the observation efficiency includes using the cable posterior from an initial run to guide observations on a return journey along the cable in the reverse direction to observe any missed cable sections. This method will also be implemented on the Smarty200 AUV operated by the University of Southampton and tested at sea to survey a prior path displaced by a specified distance from an actual subsea cable route.

#### REFERENCES

- [1] S. T. Forum, *Submarine Telecoms Industry Report Issue 12*. Submarine Telecoms Forum, Inc., 2024.
- [2] A. Mauldin, "Cable breakage: When and how cables go down."
- [3] B. Thornton, A. Bodenmann, M. M. Campos, S. Simmons, S. Gourvenec, D. White, T. Bennets, and D. Newborough, "Autonomous robotic monitoring of subsea communication cables," in *Underwater Defence Technology 2024 (09/04/24 - 11/04/24)*, April 2024.
- [4] I. Kogan, C. K. Paull, L. A. Kuhnz, E. J. Burton, S. Von Thun, H. Gary Greene, and J. P. Barry, "Atoc/pioneer seamount cable after 8 years on the seafloor: Observations, environmental impact," *Continental Shelf Research*, vol. 26, no. 6, pp. 771–787, 2006.

- [5] A. Balasuriya and T. Ura, "Vision-based underwater cable detection and following using AUVs," in *OCEANS '02 MTS/IEEE*, vol. 3, pp. 1582–1587 vol.3, Oct 2002.
- [6] A. V. Inzartsev and A. M. Pavin, "AUV cable tracking system based on electromagnetic and video data," in *OCEANS 2008 - MTS/IEEE Kobe Techno-Ocean*, pp. 1–6, 2008.
- [7] S. Thrun, W. Burgard, and D. Fox, "The GraphSLAM algorithm," in *Probabilistic Robotics*, pp. 337–383, Cambridge, MA: MIT Press, 2006.
- [8] A. Bodenmann, I. Djauhari, J. Devgon, and B. Thornton, "Real-time subsea communication cable detection for auv-based inspection," in *AUV 2024 (18/09/24 - 20/09/24)*, September 2024.
- [9] T. Yamada, A. Prügel-Bennett, and B. Thornton, "Learning features from georeferenced seafloor imagery with location guided autoencoders," *Journal of Field Robotics*, vol. 38, pp. 52 – 67, 2020.